

## Record-high hyperpolarizabilities in conjugated polymers†

Cite this: *J. Mater. Chem. C*, 2014, 2, 4533Stijn Van Cleuvenbergen,<sup>a</sup> Inge Asselberghs,<sup>ad</sup> Wouter Vanormelingen,<sup>b</sup> Thierry Verbiest,<sup>a</sup> Edith Franz,<sup>a</sup> Koen Clays,<sup>ac</sup> Mark G. Kuzyk<sup>c</sup> and Guy Koeckelberghs<sup>\*b</sup>

Disubstituted poly(phenanthrene), a conjugated polymer, has been studied by hyper-Rayleigh scattering. Although this compound lacks the donor–acceptor motif that is typically associated with a strong second-order nonlinear optical response, the (intrinsic) hyperpolarizability ranks among the highest ever measured, breaking the longstanding apparent limit. The linear and nonlinear optical properties of the polymer depend strongly on the solvent conditions, affecting the macromolecular organization. An explanation for these unexpected results is postulated and is based on modulation of conjugation along the polymer backbone. As the molecular structure of the compound does not at all fit into the classical paradigms, our observations put these theories into perspective.

Received 26th March 2014  
Accepted 24th April 2014

DOI: 10.1039/c4tc00616j

www.rsc.org/MaterialsC

## 1. Introduction

For over two decades, efforts have focused on the design of molecules to improve their nonlinear optical (NLO) behavior for various applications.<sup>1–3</sup> For second-order NLO applications, these molecules typically have a D– $\pi$ –A motif, *i.e.* a conjugated  $\pi$ -system endcapped with electron donating (D) and electron accepting (A) groups. In order to maximize the hyperpolarizability ( $\beta$ ), many different combinations of donors, acceptors and conjugated  $\pi$ -systems have been studied. Although increasingly stronger donors and acceptors do not necessarily lead to a higher hyperpolarizability, an optimized D– $\pi$ –A motif is required for achieving optimal hyperpolarizabilities.<sup>4</sup>

A very common technique to measure a molecule's hyperpolarizability is hyper-Rayleigh scattering (HRS). The hyperpolarizability is in fact a tensor composed of 27 components. The actually measured hyperpolarizability using HRS ( $\beta_{\text{HRS}}$ ) is usually composed of several tensor components. In general, the HRS response of a molecule depends on both its symmetry and its electronic transitions. The former parameter governs the number of independent non-zero tensor components  $\beta_{ijk}$ , while the latter property determines their actual value. As a consequence, if one wants to compare the general second-order NLO efficiency of different molecules,  $\beta_{\text{HRS}}$  suffices.

If, however, a particular tensor component must be evaluated, the symmetry of the molecule must be known in order to calculate the magnitude of that particular component.

One must note that increasing the strength of donors and acceptors and the length of the conjugation path to optimize  $\beta$ , also affects the absorption features of a molecule. More in particular, their increase red-shifts the absorption band. Therefore, the more efficient molecules typically also show a higher  $\lambda_{\text{max}}$ . For example, up until recently, the largest hyperpolarizabilities were measured for protected polyene or thiophene-ring containing chromophores like the benchmark compound FTC (Fig. 1,  $\beta_{\text{HRS},0} = 263 \times 10^{-30}$  esu).<sup>5,6</sup>

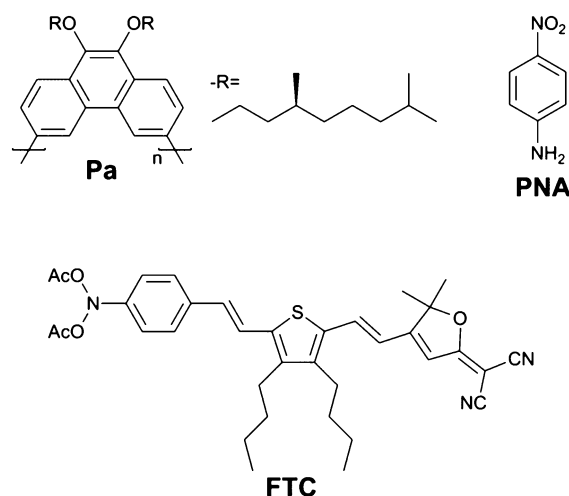


Fig. 1 Structures of the studied conjugated polymer Pa, para-nitroaniline (PNA) and benchmark compound FTC.<sup>5,6</sup>

<sup>a</sup>Laboratory of Molecular Electronics and Photonics, Katholieke Universiteit Leuven, Celestijnenlaan 200 D, B-3001 Leuven, Belgium

<sup>b</sup>Laboratory of Polymer Synthesis, Katholieke Universiteit Leuven, Celestijnenlaan 200 F, B-3001 Leuven, Belgium. E-mail: guy.koeckelberghs@chem.kuleuven.be

<sup>c</sup>Department of Physics and Astronomy, Washington State University, Pullman, USA

<sup>d</sup>IMEC, Kapeldreef 15, 3001 Leuven, Belgium

† Electronic supplementary information (ESI) available: See DOI: 10.1039/c4tc00616j

While these values are much higher than classical compounds such as *para*-nitroaniline (PNA,  $\beta_{\text{HRS},0} = 10 \times 10^{-30}$  esu),<sup>5,7</sup> the  $\lambda_{\text{max}}$  is also considerably redshifted: from 348 nm for PNA to 650 nm for FTC. This limits the window of wavelengths that can be used for applications.

In this manuscript, we report that Pa (disubstituted poly(phenanthrene), Fig. 1), a conjugated polymer which completely lacks the typical D- $\pi$ -A structure and has a rather blue-shifted absorption, shows nevertheless a record-high hyperpolarizability. An explanation is postulated to account for this unexpected result.

## 2. Experimental

### 2.1 Materials

The polymer studied (Pa) is a poly(phenanthrene) with  $\bar{M}_n = 7.3 \text{ kg mol}^{-1}$ , polydispersity = 2.5, degree of polymerization = 15. The molar mass has been measured by gel permeation chromatography (GPC) in THF towards poly(styrene) standards. Its synthesis has been described elsewhere.<sup>8</sup>

### 2.2 Methods

UV-vis and CD spectra have been recorded on a Perkin-Elmer Lambda-900 and a JASCO J810 spectrophotometer, respectively. HRS measurements have been performed at a wavelength of 800 nm. The set-up is described in full detail elsewhere.<sup>9</sup> All samples are analyzed towards crystal violet in methanol ( $\beta_{\text{HRS},800 \text{ nm}} = 208.6 \times 10^{-30}$  esu), a standard reference compound in this wavelength range. The differences in solvent and molecular symmetry between the reference and samples are accounted for by the standard local-field correction factors at optical frequencies and the appropriate factors for the contributing tensor components, respectively. To account for resonance enhancement, a static dispersion-free hyperpolarizability value ( $\beta_0$ ) is obtained using a standard two-level dispersion term.<sup>10</sup> Due to the presence of multiphoton fluorescence, the high-frequency demodulation technique has been applied to obtain fluorescence-free first hyperpolarizabilities.<sup>9,11</sup> For all solvent conditions, the HRS signal without any fluorescence contribution could be detected at a modulation frequency of 880 MHz. Depolarization measurements have been carried out at this fluorescence-free modulation frequency.

### 2.3 Theoretical calculations

To evaluate the efficiency of the second-order nonlinear optical response the polymer's intrinsic (size-independent) hyperpolarizability,  $\beta_{\text{INT}}$ , is calculated as:

$$\beta_{\text{INT}} = \frac{\beta_{\text{zzz},0}}{\beta_{\text{zzz},0,\text{MAX}}}$$

with  $\beta_{\text{zzz},0,\text{MAX}}$ :

$$\beta_{\text{zzz},0,\text{MAX}} = 3^{1/4} \left( \frac{e\hbar}{\sqrt{m}} \right)^3 \frac{N_{\pi e}^{3/2}}{E_{10}^{7/2}}$$

$N_{\pi e}$  is the effective number of polarizable electrons,  $m$  the electron mass and  $E_{10}$  the energy difference between the ground and first excited state, proportional to the reciprocal of  $\lambda_{\text{max}}$ .<sup>12</sup> For Pa the number of polarizable electrons is 210, or 14 electrons per monomeric unit.

## 3. Results and discussion

Pa adopts an unordered, coiled conformation in a good solvent such as  $\text{CHCl}_3$ , in which chirality is not expressed, and folds into a helical conformation upon decreasing the solvent quality by addition of a nonsolvent, such as hexane or methanol.<sup>8</sup> The transition to the helical conformation is accompanied by the occurrence of circular dichroism (CD), as depicted in Fig. 2. The conjugation length, however, is less affected by this transition and remains rather short, as is evidenced by its  $\lambda_{\text{max}}$ , which is a measure of conjugation length ( $\sim 360 \text{ nm}$  vs.  $321 \text{ nm}$  for the monomer).

Pa shows a very large HRS response, which strongly depends on the solvent composition (Table 1). The measurements are performed at 800 nm with  $\lambda_{\text{max}}$  similarly remote from the

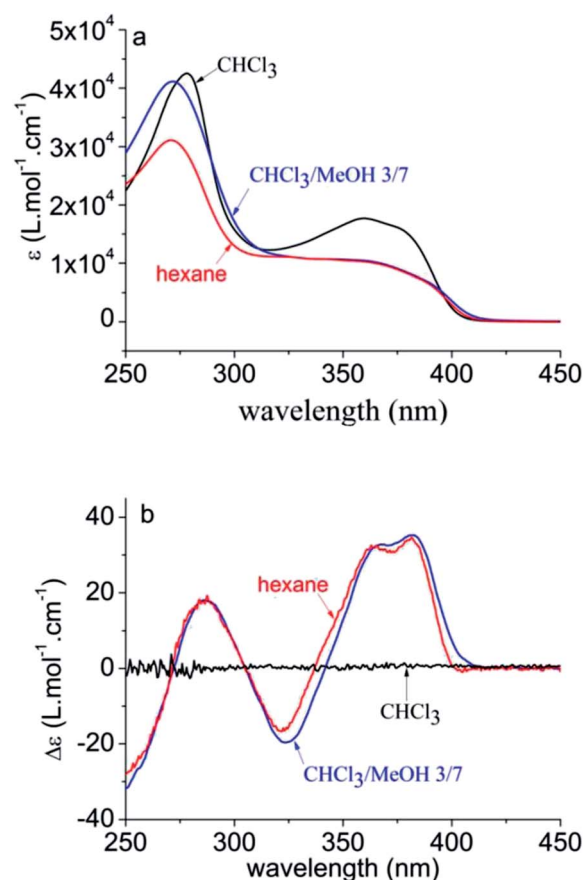


Fig. 2 UV-vis (a) and CD (b) spectra of Pa in different solvent conditions, evidencing the transition from coiled to helical conformation for poor solvents. The broad HOMO-LUMO ( $\pi$ - $\pi^*$ ) transition around 360 nm shows vibronic fine structure, as does the monomer (see ESI†). The used concentrations are  $22 \text{ mg L}^{-1}$  in  $\text{CHCl}_3$  and  $\text{CHCl}_3$ -MeOH 3/7, and  $27 \text{ mg L}^{-1}$  in hexane.



**Table 1**  $\lambda_{\max}$  is given for the HOMO–LUMO transition. Static hyperpolarizabilities are calculated using a two-level model dispersion term.<sup>10</sup> For an octupolar molecule,  $\beta_{xyz}$  is calculated from  $(\beta_{\text{HRS}})^2 = (20/35) \cdot \beta_{xyz}^2$ . For molecules of  $C_{2v}$  symmetry, like the monomer, the maximal  $\beta_{\text{INT}}$  corresponds to polar compounds with a dominant  $\beta_{zzz}$  component and is hence calculated from  $(\beta_{\text{HRS}})^2 = (6/35) \cdot \beta_{zzz}^2$ .<sup>21</sup> For all reported values, the relative experimental error is under 15%

Solvent		$\lambda_{\max}$ (nm)	$\beta_{\text{HRS},800\text{nm}}$ ( $\times 10^{-30}$ esu)	$\beta_{\text{HRS},0}$	$\beta_{xyz,0}$	$\beta_{\text{INT}}$
Pa coil (polymer)	CHCl <sub>3</sub>	360	15 000	2300	3000	$\geq 0.077$
Pa helix (polymer)	<i>n</i> -Hexane or CHCl <sub>3</sub> –CH <sub>3</sub> OH (3/7)	360	4800	730	950	$\geq 0.025$
Pa (monomer)	CHCl <sub>3</sub>	321	30	9	N/A	$< 7 \times 10^{-4}$

second-harmonic wavelength (*i.e.* 400 nm) in all conditions. The results are thus similarly affected by resonance enhancement or re-absorption. For both the samples and the reference, a series of 5 dilute concentrations has been measured. The linear increase of the second-harmonic signal with the sample concentration shows that the results are not influenced by aggregation of the polymer.  $\beta_{\text{HRS},0}$  in CHCl<sub>3</sub>, in which the polymer adopts a disordered coil-state, amounts to  $2300 \times 10^{-30}$  esu, while in hexane or CHCl<sub>3</sub>–CH<sub>3</sub>OH mixture, in which a helix is formed,  $\beta_{\text{HRS},0}$  amounts to  $730 \times 10^{-30}$  esu. The monomer itself, measured in chloroform, has a static hyperpolarizability of  $9 \times 10^{-30}$  esu, and therefore can on its own not account for the large NLO response of the polymer. If these values are compared with that of the classical D– $\pi$ –A chromophore PNA ( $\beta_{\text{HRS},0} = 10 \times 10^{-30}$  esu), which has a similar  $\lambda_{\max}$ , it is clear that Pa is orders of magnitude stronger.<sup>7</sup> Even the benchmark chromophore FTC ( $\beta_{\text{HRS},0} = 263 \times 10^{-30}$  esu), is outperformed by Pa.

One might argue that the large response stems mainly from the substantial number of  $\pi$ -electrons. Indeed, it is evident that for an optimized system, the magnitude of the response increases with the number of polarizable electrons. Thus, to evaluate or compare the intrinsic efficiency of different compounds, the number of polarizable electrons must be accounted for. In first approximation, this is often done by scaling  $\beta_{\text{HRS},0}$  towards the number of  $\pi$ -electrons ( $\beta_{\text{HRS},0}/N_{\pi e}$ ). Even if the number of polarizable electrons is taken into account, Pa compares to the best traditional D– $\pi$ –A chromophores.<sup>13–20</sup> For example,  $\beta_{\text{HRS},0}/N_{\pi e}(\text{FTC}) = 10 \times 10^{-30}$  esu, while  $\beta_{\text{HRS},0}/N_{\pi e}(\text{Pa}) = 11 \times 10^{-30}$  esu. Note that in these calculations,  $N_{\pi e}$  of Pa is calculated based on the  $M_n$  obtained by GPC, which typically overestimates the molar mass of conjugated polymers.

Apart from  $\beta_{\text{HRS}}$  or  $\beta_{\text{HRS},0}/N_{\pi e}$ , the NLO efficiency of molecules can also be compared more rigorously by their intrinsic (size-independent) hyperpolarizability ( $\beta_{\text{INT}}$ ), as defined by Kuzyk.<sup>22</sup> This model uses Thomas-Kuhn sum rules to estimate a compound's maximum molecular first hyperpolarizability,  $\beta_{\text{MAX}}$ , and defines  $\beta_{\text{INT}}$  as the ratio of the experimentally determined static hyperpolarizability,  $\beta_0$  over the maximum molecular hyperpolarizability.

In 2004 a survey of the best chromophores up until then revealed that, despite the progress made in achieving ever higher hyperpolarizabilities, their intrinsic hyperpolarizabilities all fall a

factor  $10^{-3/2}$  short of the fundamental limit (*i.e.* when  $\beta_{\text{INT}}$  is 1).<sup>23</sup> Since it has been shown that this limit is not of a fundamental nature, it has been recognized as the *apparent* limit. Indeed, from 2007 on there have been reports of molecules breaching this limit.<sup>13,24–26</sup>

Since  $\beta_{\text{MAX}}$  can be calculated for the *zzz*-component but not for the overall  $\beta_{\text{HRS}}$ ,  $\beta_{zzz,0}$  must be known. As already mentioned, this requires that the actual symmetry of the molecules is known. Applied to Pa, the symmetry of the particular random coil is unknown and in principle all tensor components can contribute. The  $C_2$  symmetry of a helix, on the other hand, restricts the number of independent, nonvanishing tensor components to four,  $\beta_{xyz}$ ,  $\beta_{yxx}$ ,  $\beta_{yzz}$ , and  $\beta_{yyy}$ .<sup>27,28</sup> In order to determine the number of actually contributing tensor components, depolarization measurements were performed. The depolarization ratio,  $\rho$ , which is the ratio of the horizontal to vertical polarized second harmonic light intensity with respect to the vertical input polarization, amounts to 0.68 in all solvent conditions. In combination with the macromolecular topology, this reveals that only octupolar contributions<sup>27,28</sup> contribute to the HRS-response and that therefore  $\beta_{xyz}$  is the only relevant tensor component in all solvent conditions. As a consequence,  $\beta_{xyz,0}$ , expressed per polymer, is calculated from all HRS measurements and amounts to  $3000 \times 10^{-30}$  esu in CHCl<sub>3</sub> and  $950 \times 10^{-30}$  esu in hexane and CHCl<sub>3</sub>–methanol (3/7).  $\beta_{zzz,\text{MAX}}$  amounts to  $43\,000 \times 10^{-30}$  esu in all solvent conditions. Since  $\beta_{xyz,\text{MAX}} \leq \beta_{zzz,\text{MAX}}$ <sup>29</sup> it can be concluded that  $\beta_{\text{INT}} \geq 0.077$  (coil) and  $\beta_{\text{INT}} \geq 0.025$  (helix), revealing record-high  $\beta_{\text{INT}}$  and breaking the apparent limit in the coiled conformation. Note that the assumptions that have been made in order to calculate  $\beta_{\text{INT}}$  each underestimate  $\beta_{\text{INT}}$ . Indeed, the first assumption is  $\beta_{xyz,\text{MAX}} \leq \beta_{zzz,\text{MAX}}$ . Second,  $N_{\pi e}$  is estimated from  $M_n$  measured by GPC. This technique typically overestimates the molar mass of conjugated polymers and, consequently,  $\beta_{\text{MAX}}$  will be overestimated as well. As a consequence, the actual  $\beta_{\text{INT}}$  is likely to be even higher than the one tabulated. We must finally mention that, while classical chromophores are typically rigid molecules with a fixed conformation (and hyperpolarizability), this is not at all the case for Pa. In contrast, the polymer molecules can adopt many different conformations, each with a different hyperpolarizability. Since an averaged hyperpolarizability is measured, this implies that some molecules display a hyperpolarizability which is even higher than the one calculated. Indeed, Méreau *et al.* have



demonstrated that the hyperpolarizability in a dynamic structure significantly depends on the actual conformation.<sup>30</sup>

It is clear that Pa shows a record-high hyperpolarizability, regardless of the criterion used. This opens of course the question what the origin of this phenomenon is. A clue to this question can be found in the evolution of the hyperpolarizability and the UV-vis and CD spectra upon decreasing the solvent quality. For this purpose, the following parameters were defined and plotted (Fig. 3c and d):

$$x_{UV-vis} = \frac{\epsilon_{CHCl_3,358nm} - \epsilon_{358nm}}{\epsilon_{CHCl_3,358nm} - \epsilon_{helix,358nm}}$$

$$x_{CD} = \frac{\Delta\epsilon_{382nm}}{2\Delta\epsilon_{helix,382nm}} + \frac{\Delta\epsilon_{323nm}}{2\Delta\epsilon_{helix,323nm}}$$

$$x_{HRS} = \frac{\beta_{xyz,CHCl_3} - \beta_{xyz}}{\beta_{xyz,CHCl_3} - \beta_{xyz,helix}}$$

in which the “helix” conditions refer to CHCl<sub>3</sub>–methanol (3/7) or hexane. These parameters reflect the stepwise transformation from the coiled ( $x = 1$ ) to the helical conformation ( $x = 0$ ). The evolution of the CD and UV-vis spectra depends on the amount of (one-handed) helices and therefore probes the coil-helix transition and the change in conjugation related with it.

In all solvent conditions, also in the intermediate mixtures,  $\rho$  is unaffected. Therefore,  $\beta_{xyz}$  remains the sole important contribution to the HRS response in all conditions. As a consequence, the evolution of the HRS intensity in different solvent conditions cannot be ascribed to a symmetry change, which might affect the number of nonzero-components, but must originate from a different magnitude of  $\beta_{xyz}$ . The magnitude of the hyperpolarizability is affected by the transition dipole moment of the HOMO–LUMO transition, which is proportional to the strength of the peak in the extinction spectrum. Although the HOMO–LUMO band becomes weaker upon addition of nonsolvent, it is apparent that this change in

absorption does not coincide with the measured  $\beta_{xyz}$  values (Fig. 3). This implies that the change in transition dipole moment cannot solely explain the evolution of the hyperpolarizability in different solvent conditions.

For certain chiral systems, magnetic dipole interactions have to be included to accurately describe the NLO response. Indeed, strong delocalization of electrons in helical structures can induce magnetization, contributing to the hyperpolarizability of the polymer. This contribution is generally small, although measurements in the solid phase demonstrate that in some cases the magnitude of magnetic dipole components cannot be neglected.<sup>31,32</sup> However, if the same experiment is repeated with a poly(phenanthrene) analogue substituted with achiral *n*-octyl groups, the CD response vanishes and similar results are obtained.<sup>33</sup> Moreover, the fact that the HRS curve does not coincide with the CD and UV-vis curves, demonstrates that the HRS response is not determined by the ratio of coil/helix. The increase of the HRS signal at low methanol content is exemplary in this respect. In these conditions, no helices are yet formed and the conjugation length does not change (as shown by the CD and UV-vis spectra), but the HRS response changes. We conclude that neither helix formation, nor intrinsic chirality is required for a large second-order NLO response.

Other possible phenomena that can contribute to the measured second-harmonic response of Pa relate to short-range molecular interactions within the polymer chain, *e.g.* between different parts showing strong conjugation. Firstly, statistically dependent positional and orientational correlations between different sections along the polymer chain can give rise to coherent HRS.<sup>34,35</sup> The total second-harmonic amplitude is then found as the coherent sum over these correlated sections. A second effect can be linked with the temporally and spatially fluctuating molecular field  $F$ , which becomes important in regions of near-range ordering.<sup>36–39</sup> The low-frequency ( $\sim$ dc) molecular field then gives rise to electric-field induced second-harmonic generation (EFISHG), in which case the contribution of the second hyperpolarizability  $\gamma_{ijkl}$  should be considered and  $\beta_{ijk}$  becomes proportional to  $\gamma_{ijkl}F$ . Since this is in essence a third-order NLO process, this phenomenon also occurs for centrosymmetric molecules. However, in the limited amount of experimental studies on the subject this effect is found to be non-negligible but rather weak.<sup>36–38,40</sup> Moreover, it is important to note that molecular correlations and interactions not only change the intensity, but also the polarization dependence, *i.e.* the depolarization ratio  $\rho$ , of HRS light.<sup>35–37</sup> This effect has been exploited in several studies to investigate molecular correlations between chromophores or to determine the contribution of the local molecular field  $F$ .<sup>36–38,41–44</sup> For Pa however, the depolarization ratio remains constant for different solvent conditions while the intensity changes drastically, implying that short-range interactions at least cannot explain the evolution of  $\beta_{xyz}$ .

Importantly, addition of nonsolvent does influence the torsion angle  $\theta$  between the consecutive phenanthrene units. Indeed, this induces a shrinking of the (coiled) polymer chains upon which a helical conformation is formed. Both processes – the shrinking of the coils and the formation of a helix – alter  $\theta$  and, consequently, the conjugation.

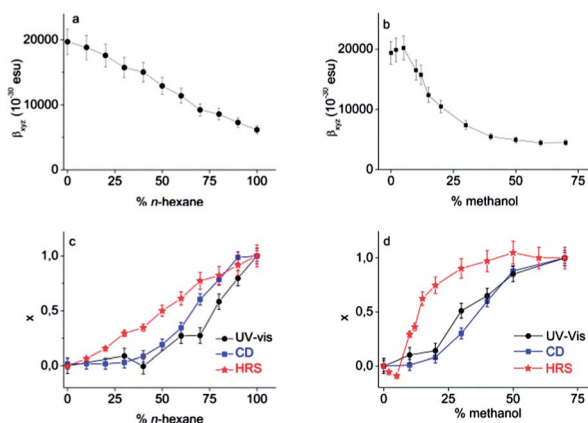


Fig. 3  $\beta_{HRS}$  in chloroform mixtures upon addition of (a) *n*-hexane and (b) methanol. Relative evolution of the coil  $\rightarrow$  helix transition probed by UV-vis and CD spectroscopy and HRS in chloroform upon addition of (c) *n*-hexane and (d) methanol ( $c = 92 \text{ mg L}^{-1}$ ).



We hypothesize that this extraordinary high hyperpolarizability relates to the theoretical findings of Kuzyk and coworkers. Their extensive numerical calculations point out that optimal hyperpolarizabilities are reached by effectively varying the potential energy landscape of the  $\pi$ -conjugation.<sup>45–47</sup> It must be mentioned that a complete breaking of the conjugation ( $\theta = 90^\circ$ ) is naturally also detrimental. Optimal hyperpolarizabilities are expected in molecules with strong, but varying conjugation. The evolution of the hyperpolarizability in different solvent conditions can then be explained by a change in  $\theta$ , modulating conjugation and resulting in possibly extremely efficient chromophores. These calculations also suggest that enhanced hyperpolarizabilities, alongside optimized variation of the potential energy landscape, require the presence of two dominant electronic transitions.<sup>47</sup> This seems to be in line with the absorption spectrum of Pa with one transition around 275 nm and one near 360 nm. These spectral features are in fact common to all conjugated polymers and are ascribed to absorption of the monomer unit for the short wavelength band, and a  $\pi$ - $\pi^*$  transition of the delocalized conjugated system along the polymer backbone for the HOMO–LUMO band. Interestingly, substantial hyperpolarizabilities were recently also measured in poly(3-alkylthiophene)s.<sup>48</sup>

Again, there have been some reports in recent years of molecules breaking the apparent limit. It must be noted that these molecules also obey the principle of potential energy modulation, either by combining groups with different effective conjugation<sup>13</sup> or by tuning the angle between the electron donating moiety and the  $\pi$ -conjugated bridge.<sup>25</sup> Importantly, these reports concern D- $\pi$ -A molecules, while Pa does not show this typical D- $\pi$ -A motif at all. Our results clearly deny the necessity of an electron donating and withdrawing moiety, *i.e.* the typical D- $\pi$ -A structure, for achieving a high hyperpolarizability. As mentioned, a recent study has demonstrated that poly(3-alkylthiophene)s, despite the limited donor strength of the alkyl substituents, display a large second-order NLO response, be it substantially lower than Pa.<sup>48</sup> Also, several reports showed that an octupolar symmetry by itself, even in absence of a D- $\pi$ -A motif, can result in a substantial second-order NLO response.<sup>49–51</sup> Indeed, such a D- $\pi$ -A motif is one, but not the only way to provide the (i) required noncentrosymmetry and (ii) the conjugation modulation. The magnitude of the hyperpolarizability in Pa puts the importance of a D- $\pi$ -A structure with  $C_{2v}$  symmetry into perspective with respect to other symmetry-breaking paradigms, such as torsion between conjugated planes, resulting in  $D_2$  symmetry.<sup>52</sup> Importantly, while D- $\pi$ -A molecules typically concern planar molecules in order to maximize conjugation, efficient potential energy fluctuations are not favored in such flat molecules.

## 4. Conclusions

In conclusion, we have demonstrated that Pa, a conjugated polymer that lacks the push–pull (D- $\pi$ -A) substitution pattern typically associated with strong NLO compounds, unexpectedly shows an extremely high hyperpolarizability. Even after scaling the NLO response to the number of polarizable electrons, by

calculating the (size-independent) intrinsic hyperpolarizability, Pa ranks among the best chromophores ever measured. Indeed, it is one of the few compounds breaking the longstanding apparent limit, and is to the best of our knowledge the first compound that achieves this without relying on the traditional D- $\pi$ -A design.

The macromolecular conformation is found to be strongly dependent on the solvent conditions, evolving from an unordered coiled to a helical conformation upon addition of non-solvent, as evidenced by CD and UV-vis spectroscopy. We found the largest  $\beta_{\text{INT}}$  for the unordered coiled conformation, evidencing that chirality is not required for obtaining a large NLO response in this system. While the hyperpolarizability is dependent on the solvent conditions, it does not correlate clearly with the ratio helix/coil found in different solutions. Rather, depolarization measurements point out that the NLO response is governed by octupolar contributions for both the helical and the coiled state. In line with recent theoretical and experimental findings, we postulate that the variation in second-order NLO intensity upon addition of nonsolvent is related to modulation of conjugation along the polymer backbone, by influencing the torsion angle between consecutive phenanthrene units, and resulting in extremely efficient chromophores.

These unexpected results can lead to new insights for the design of efficient second-order NLO materials and put the common molecular design paradigms into perspective. In particular, the use of 3D macromolecules that allow for an efficient modulation of conjugation is an interesting path to explore. Additionally, the octupolar character of the second-order NLO response in Pa can be particularly attractive for the development of polarization-insensitive devices, while the limited conjugation length ensures transparency in the visible region. Further research will focus on the exact influence of the conformation of conjugated polymers on their hyperpolarizability and on determining the properties of the solid state. In this respect, it is important to note that aggregation in the solid state undoubtedly affects the conformation and hence the hyperpolarizability of the polymer. The fact that the actual hyperpolarizability of the polymer is, with the assumptions made, underestimated and the fact that an averaged hyperpolarizability of a broad scale of different conformations with different hyperpolarizability is measured, leaves the possibility to further increase the hyperpolarizability of conjugated polymers.

## Acknowledgements

We acknowledge Dr Javier Pérez-Moreno for the fruitful discussions. We are grateful to the University of Leuven (GOA) and the Fund for Scientific Research (FWO-Vlaanderen) for financial support. MGK thanks the National Science Foundation (ECS-1128076).

## Notes and references

- 1 P. N. Prasad and D. J. Williams, *Introduction to Nonlinear Optical Properties of Molecules and Polymers*, 1991.



- 2 T. Verbiest, S. Houbrechts, M. Kauranen and K. Clays, *J. Mater. Chem.*, 1997, **7**, 2175–2189.
- 3 L. R. Dalton, W. H. Steier, B. H. Robinson, C. Zhang, A. Ren, S. Garner, A. Chen, T. Londergan, L. Irwin, B. Carlson, L. Fifield, G. Phelan, C. Kincaid, A. Jen, S. California and L. Angeles, *J. Mater. Chem.*, 1999, **9**, 1905–1920.
- 4 S. R. Marder, B. Kippelen, A. K.-Y. Jen and N. Peyghambarian, *ChemInform*, 2010, **28**, 845–851.
- 5 PNA = *p*-nitroaniline; FTC = 2-dicyanomethylen-3-cyano-4-[2-[*trans*-[4-(*N,N*-diacetoxyethylamino)]phenylene-3,4-dibutylthienyl-5]ethynylene]-5,5-dimethyl-2,5-dihydrofuran.
- 6 Y. Shi, C. Zhang, H. Zhang, J. H. Bechtel, L. Dalton, B. H. Robinson and W. H. Steier, *Science*, 2000, **288**, 119–122.
- 7 P. Kaatz and D. Shelton, *J. Chem. Phys.*, 1996, **105**, 3918–3929.
- 8 W. Vanormelingen, A. Smeets, E. Franz, I. Asselberghs, K. Clays, T. Verbiest and G. Koeckelberghs, *Macromolecules*, 2009, **42**, 4282–4287.
- 9 G. Olbrechts, R. Strobbe, K. Clays and A. Persoons, *Rev. Sci. Instrum.*, 1998, **69**, 2233–2241.
- 10 J. Oudar and D. Chemla, *J. Chem. Phys.*, 1977, **66**, 2664–2668.
- 11 G. Olbrechts, K. Wostyn, K. Clays and A. Persoons, *Opt. Lett.*, 1999, **24**, 403–405.
- 12 M. G. Kuzyk, *J. Mater. Chem.*, 2009, **19**, 7444.
- 13 J. Pérez-Moreno, Y. Zhao, K. Clays and M. G. Kuzyk, *Opt. Lett.*, 2007, **32**, 59–61.
- 14 J.-M. Raimundo, P. Blanchard, N. Gallego-Planas, N. Mercier, I. Ledoux-Rak, R. Hierle and J. Roncali, *J. Org. Chem.*, 2002, **67**, 205–218.
- 15 J. Luo, Y.-J. Cheng, T.-D. Kim, S. Hau, S.-H. Jang, Z. Shi, X.-H. Zhou and A. K.-Y. Jen, *Org. Lett.*, 2006, **8**, 1387–1390.
- 16 B. H. Robinson, L. R. Dalton, A. W. Harper, A. Ren, F. Wang, C. Zhang, G. Todorova, M. Lee, R. Aniszfeld, S. Garner, A. Chen, W. H. Steier, S. Houbrecht, A. Persoons, I. Ledoux, J. Zyss and A. K. Y. Jen, *Chem. Phys.*, 1999, **245**, 35–50.
- 17 Y. Liao, B. E. Eichinger, K. A. Firestone, M. Haller, J. Luo, W. Kaminsky, J. B. Benedict, P. J. Reid, A. K.-Y. Jen, L. R. Dalton and B. H. Robinson, *J. Am. Chem. Soc.*, 2005, **127**, 2758–2766.
- 18 P. Y. Moh, P. Cubillas, M. W. Anderson and M. P. Atfield, *J. Am. Chem. Soc.*, 2011, **133**, 13304–13307.
- 19 C. Cai, I. Liakatas, M. Wong, M. Bo, C. Bosshard, P. Gu, S. Concilio, N. Tirelli and U. W. Suter, *Org. Lett.*, 1999, **1**, 1847–1849.
- 20 M. G. Kuzyk, *Characterization Techniques and Tabulations for Organic Nonlinear Optical Materials*, Taylor & Francis, 1998.
- 21 T. Verbiest, K. Clays and V. Rodriguez, *Second-order Nonlinear Optical Characterization Techniques: An Introduction*, 2009.
- 22 M. G. Kuzyk, *J. Mater. Chem.*, 2009, **19**, 7444.
- 23 K. Tripathy, J. P. Moreno, M. G. Kuzyk, B. J. Coe, K. Clays and A. M. Kelley, *J. Chem. Phys.*, 2004, **121**, 7932–7945.
- 24 J. Pérez-Moreno, Y. Zhao, K. Clays, M. G. Kuzyk, Y. Shen, L. Qiu, J. Hao and K. Guo, *J. Am. Chem. Soc.*, 2009, **131**, 5084–5093.
- 25 H. Kang, A. Facchetti, H. Jiang, E. Cariati, S. Righetto, R. Ugo, C. Zuccaccia, A. Macchioni, C. L. Stern, Z. Liu, S.-T. Ho, E. C. Brown, M. A. Ratner and T. J. Marks, *J. Am. Chem. Soc.*, 2007, **129**, 3267–3286.
- 26 H. Kang, A. Facchetti, P. Zhu, H. Jiang, Y. Yang, E. Cariati, S. Righetto, R. Ugo, C. Zuccaccia, A. Macchioni, C. L. Stern, Z. Liu, S. Ho and T. J. Marks, *Angew. Chem., Int. Ed.*, 2005, **44**, 7922–7925.
- 27 J. Zyss, *J. Chem. Phys.*, 1993, **98**, 6583.
- 28 P. D. Maker, *Phys. Rev. A*, 1970, **1**, 923–951.
- 29 M. G. Kuzyk, *IEEE J. Sel. Top. Quantum Electron.*, 2001, **7**, 774–780.
- 30 R. Méreau, F. Castet, E. Botek and B. Champagne, *J. Phys. Chem. A*, 2009, **113**, 6552–6554.
- 31 M. Kauranen, T. Verbiest, E. W. Meijer, E. E. Havinga, M. N. Teerenstra, A. J. Schouten, R. J. M. Nolte and A. Persoons, *Adv. Mater.*, 1995, **7**, 641.
- 32 T. Verbiest, S. Van Elshocht, M. Kauranen, L. Hellemans, J. Snauwaert, C. Nuckolls, T. J. Katz and A. Persoons, *Science*, 1998, **282**, 913–915.
- 33  $\beta_{xyz,0}$  amounts to  $1800 \times 10^{-30}$  esu in pure  $\text{CHCl}_3$ , and to  $760 \times 10^{-30}$  esu in  $\text{CHCl}_3\text{-MeOH}$  (5/5).
- 34 S. Kielich, *Acta Phys. Pol., A*, 1974, **45**, 231–251.
- 35 D. P. Shelton, *J. Chem. Phys.*, 2013, **138**, 154502.
- 36 S. Kielich, J. Lalanne and F. Martin, *Phys. Rev. Lett.*, 1971, **26**, 1295–1298.
- 37 S. Kielich, *J. Raman Spectrosc.*, 1973, **1**, 119–139.
- 38 J. Lalanne, F. Martin and S. Kielich, *Chem. Phys. Lett.*, 1975, **30**, 73–76.
- 39 S. N. Yaliraki and R. J. Silbey, *J. Chem. Phys.*, 1999, **111**, 1561.
- 40 D. P. Shelton, *J. Chem. Phys.*, 2009, **130**, 114501.
- 41 J. Chen and K. Y. Wong, *J. Chem. Phys.*, 2005, **122**, 174505.
- 42 Y. C. Chan and K. Y. Wong, *J. Chem. Phys.*, 2012, **136**, 174514.
- 43 D. P. Shelton, *J. Chem. Phys.*, 2013, **138**, 054502.
- 44 D. P. Shelton, *J. Chem. Phys.*, 2010, **133**, 234507.
- 45 J. Zhou, M. G. Kuzyk and D. S. Watkins, *Opt. Lett.*, 2006, **31**, 2891–2893.
- 46 S. Shafei, M. C. Kuzyk and M. G. Kuzyk, *J. Opt. Soc. Am. B*, 2010, **27**, 1849.
- 47 J. Zhou, U. Szafruga, D. Watkins and M. Kuzyk, *Phys. Rev. A: At., Mol., Opt. Phys.*, 2007, **76**, 053831.
- 48 S. Deckers, S. Vandendriessche, D. Cornelis, F. Monnaie, G. Koeckelberghs, I. Asselberghs, T. Verbiest and M. A. van der Veen, *Chem. Commun.*, 2014, **50**, 2741–2743.
- 49 S. Van Cleuvenbergen, I. Asselberghs, E. M. García-Frutos, B. Gómez-Lor, K. Clays and J. Pérez-Moreno, *J. Phys. Chem. C*, 2012, **116**, 12312–12321.
- 50 R. Jua, M. Ramos, J. L. Segura, S. Van Cleuvenbergen, K. Clays, T. Goodson, J. T. Lo and J. Casado, *J. Phys. Chem. C*, 2013, **117**, 626–632.
- 51 M. Quintiliani, J. Pérez-Moreno, I. Asselberghs, P. Vázquez, K. Clays and T. Torres, *J. Phys. Chem. B*, 2010, **114**, 6309–6315.
- 52 T. V. Duncan, K. Song, S.-T. Hung, I. Miloradovic, A. Nayak, A. Persoons, T. Verbiest, M. J. Therien and K. Clays, *Angew. Chem., Int. Ed.*, 2008, **47**, 2978–2981.

